

Pervasive electronic nematicity in a cuprate superconductor

J. Wu^a, A.T. Bollinger^a, X. He^{a,b}, I. Božović^{a,b,*}

^a Brookhaven National Laboratory, Upton, NY 11973-5000, USA

^b Yale University, Applied Physics Department, New Haven, CT 06520, USA



ARTICLE INFO

Keywords:

High-temperature superconductivity
Cuprates
Molecular beam epitaxy
Superfluid density
Electronic nematicity

ABSTRACT

We describe an extensive experimental study of $\text{La}_{2-x}\text{Sr}_x\text{CuO}_4$ films synthesized by molecular beam epitaxy and investigated by angle-resolved measurements of transverse resistivity (without applied magnetic field). The data show that an unusual metallic state, in which the rotational symmetry of the electron fluid is spontaneously broken, occurs in a large temperature and doping region. The superconducting state always emerges out of this nematic metal state.

1. Background and motivation

Since its discovery in the 1980s, understanding the high temperature superconductivity (HTS) in cuprates has been the foremost open problem in condensed matter physics. Even the most basic premises are still forcefully debated. One key question is whether the superconducting state conforms to the standard Bardeen–Cooper–Schrieffer (BCS) theory. Another is on whether (and where in the doping–temperature phase diagram) the metallic ‘normal’ state complies with the standard Drude–Lorentz–Sommerfeld–Landau picture. These two questions are related: in the BCS picture, the formation of Cooper pairs is a result of the instability of the Fermi liquid upon cooling.

To address these two questions, we have performed a comprehensive set of experiments in which over 2000 films of $\text{La}_{2-x}\text{Sr}_x\text{CuO}_4$ (LSCO) are studied in great detail. We have found that in LSCO, on the overdoped side, the superconducting transition temperature T_c scales with the superfluid density [1], in variance with the predictions from BCS theory [2]. Next, we have observed that the electric transport spontaneously breaks the fourfold rotation symmetry of the underlying crystal [3]. The electron fluid has intrinsic anisotropy, and behaves like a Fermi Liquid Crystal. This ‘electronic nematicity’ has been anticipated theoretically [4–12], and observed experimentally in earlier (magneto) transport, Nernst effect, scanning tunneling microscopy, Raman spectroscopy, THz polarimetry and thermal conductivity studies [13–23]. A new result in our work is that we observe nematicity in a broad range of temperature (T) and doping levels (labeled here by the carrier density p); the superconducting state always emerges out of the nematic metal state (or vice versa). Moreover, we show that the nematic director orientation depends on both T and p .

2. How to search for nematicity: angle-resolved transverse resistivity measurements

To check whether the electron transport breaks the fourfold crystal symmetry—the electronic nematicity—the first that comes to mind is to measure the longitudinal resistivity along different crystal axes. For instance, one can simply measure the longitudinal voltages by applying an excitation current along the a and b in-plane axes of the LSCO crystal lattice respectively, and retrieve the corresponding resistivity ρ_a and ρ_b . If the nematic director is aligned with either the a or b axis, the magnitude of nematicity can be defined as $N = |\rho_a - \rho_b| / (\rho_a + \rho_b)$. The sensitivity of this method is determined by the accuracy in extracting the difference between ρ_a and ρ_b . If this difference is substantial (as for the case of very underdoped LSCO), this approach works well. However, it may fail to detect a small degree of anisotropy. First, this is limited by uncertainty in the sample geometry; even when in thin films the devices are defined by lithography, one can expect a few per cent variations and scatter, and typically even more when the contacts are painted or evaporated on bulk crystals. Moreover, the longitudinal resistivity ρ is the sum of the contributions from multiple sources, e.g. the defect scattering, the electron–phonon scattering, the electron–electron scattering, etc. The signal that originates from electronic nematicity thus may be mixed up with other sources, and is superposed onto a large background. This sets the limit of the sensitivity in N to be about 5%. As we will show below, this is not sufficient to detect the nematicity in optimally doped and overdoped films, and this may be the reason why no electronic nematicity was reported at these doping levels in the literature.

The alternative approach that we proposed is to measure the off-diagonal elements of the resistivity/conductivity tensor, i.e., to measure

* Corresponding author at: Brookhaven National Laboratory, Upton, NY 11973-5000, USA.
E-mail address: bozovic@bnl.gov (I. Božović).

the voltage V_T transverse to the current I direction. In a tetragonal material, V_T should be strictly zero by (the C_{4v} point group) symmetry. A non-zero V_T could only occur if the symmetry is broken, e.g. by an external magnetic field as in the Hall effect, or by an internal (real or ‘virtual’) field as in the anomalous Hall effect. If the electron transport has orthorhombic (or lower) symmetry, a non-zero V_T must occur; in fact, it must oscillate as $V_T^0 \sin(2\phi)$ as a function of the azimuth angle ϕ .

To factor out the geometrical parameters, we define the transverse resistivity $\rho_T \equiv (V_T/I)t$ where t is the film thickness. Measuring ρ_T is a very sensitive probe for electronic nematicity, orders of magnitude higher than that of the longitudinal resistivity ρ , because the sole source of the measured ρ_T is electronic nematicity and because there is no background (it is zero by symmetry). Similar to the principle of the Wheatstone bridge method widely used to accurately measure resistance, zeroing out the background is the key to achieving a higher sensitivity. We have used the same method in the search of phase fluctuations of the charge cluster glass state in underdoped cuprates, and found that by switching the probe from ρ to the Hall resistivity ρ_H , the measurement sensitivity improved by more than three orders of magnitude [32]. This idea can be generalized to the studies of electronic nematicity with other techniques. For example, it is better to measure off-diagonal components of the reflectivity or transmissivity rather than the diagonal components to characterize the electronic nematicity. Electronic Raman continuum should show it much more pronounced in the B_{2g} geometry than in A_{1g} .

In principle, the nematicity has not only an amplitude characterized by N , but also an in-plane orientation characterized by a ‘director’ \mathbf{n} , or equivalently, by the angle α it makes with some fixed axis. Note that \mathbf{n} is not a proper unit vector, since it doesn't differentiate between two opposite directions, e.g. $[1\ 0\ 0]$ and $[-1\ 0\ 0]$. Hence, $\rho_T(\phi)$ should have the period of 180° , and must have four nodes, which is much easier to detect than a small difference between ρ_a and ρ_b .

3. Experimental

Our $\text{La}_{2-x}\text{Sr}_x\text{CuO}_4$ (LSCO) thin film samples were grown in a custom-built oxide molecular beam epitaxy (MBE) system that allows for atomic-layer-by-layer (ALL) synthesis with a high degree of control over film growth [24]. Oxidation is provided by a system that floods the region around the substrate with pure ozone. The partial pressure of the ozone is held constant at 10^{-6} Torr during the entire film synthesis. Atomic beams of La, Sr, and Cu are supplied by thermal evaporation sources that slowly deposited these elements onto the surface of heated LaSrAlO_4 (LSAO) substrates. The temperature of the substrates is held at 700°C , which is high enough to allow considerable surface mobility of the incoming atoms and yet low enough that bulk diffusion is nearly absent. A scanning quartz crystal monitor is used to determine the absolute flux rate for each source to within one per cent accuracy before each growth. During growth, the sources are held at a constant temperature ($\pm 0.1^\circ\text{C}$) so that the flux from each remains very stable ($< 1\%$ change). Pneumatically actuated shutters control the deposition time from each source. With computer control of the shuttering sequence and times, the entire deposition process is regulated very accurately, at a level of better than one percent of an atomic monolayer, consequently allowing for atomic layer-by-layer growth.

The thin film structure is monitored in real time during the growth process by reflection high energy electron diffraction (RHEED). It reveals epitaxial growth, with the Cu–O–Cu bond direction in the LSCO parallel to the Al–O–Al bond direction in LSAO. Oscillations in the RHEED intensity as each atomic layer is formed provide a digital control of the film thickness, t , which for films reported here was kept at 20 unit cells (264 \AA). After each film growth is complete, the samples were annealed in situ to control their oxygen content. Underdoped LSCO films were annealed in vacuum at 300°C for several hours, to eliminate any excess interstitial oxygen that may have been introduced during the growth. Overdoped films, on the other hand, were annealed in a partial

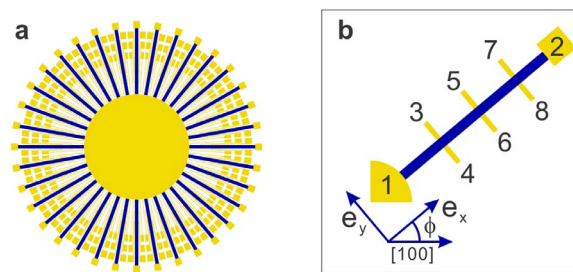


Fig. 1. (a) The ‘sunbeam’ lithography pattern. It contains 36 Hall bars and the angle between two successive bars is 10° . (b) A schematic drawing of a single Hall bar. The blue strip represents the portion of copper oxide film (‘Hall bar’) that remains after etching; yellow shapes are the gold contact pads. The probe current runs from contact 1 to 2; the transverse voltage is measured between contact pairs (3, 4), (5, 6) or (7, 8); and ϕ is the angle between the current direction and the crystallographic $[1\ 0\ 0]$ axis. (For interpretation of the references to color in this figure legend, the reader is referred to the web version of this article.)

pressure of 10^{-5} Torr of ozone to remove any oxygen vacancies.

The ALL-MBE technique solves the problems of film nucleation and phase separation, yielding atomically perfect films of HTS compounds as well as precise multilayer and superlattice heterostructures. These allow fabrication of unique devices that enable novel experiments for probing the basic physics of HTS [24–34].

For the present experiment, each film was patterned into the ‘sunbeam’ device layout (Fig. 1a) by standard micro-fabrication techniques. The geometry was defined on the film surface by photolithography and pattern transfer was accomplished by argon ion milling, with a beam voltage of 500 V and a current density of 2.5 mA/cm^2 . A double-layer resist photolithography process, electron-beam evaporation of several hundred nanometers of gold, and subsequent liftoff formed the electrical traces and contact pads. The sunbeam consists of 36 ‘rays’ with an equal angular separation of $\Delta\phi = 10^\circ$. Each ray contains a Hall bar device with three pairs of transverse contacts (Fig. 1b), which we used to study the electrical transport in our films. The bars were current biased between contacts 1 and 2, along the \hat{e}_x direction, with a current $I_x = 2\ \mu\text{A}$. This was safely in the linear regime; all voltage-current curves were linear up to at least $10\ \mu\text{A}$ for all devices and temperatures above T_c that we examined. Neighboring pairs of voltage contacts along the bar, such as 3 and 5 or 6 and 8, were used to measure the longitudinal voltage, V , and hence determine the longitudinal resistivity, ρ , for each bar. Pairs of voltage contacts opposite from one another, along the \hat{e}_y direction, such as 3 and 4 or 5 and 6, were used to measure the transverse voltage, V_T . To factor out the bias current and sample size we introduce the transverse resistivity $\rho_T \equiv (V_T/I_x)t$.

The edges of the LSAO substrates are cut and polished to be parallel to the crystallographic $[1\ 0\ 0]$, $[0\ 1\ 0]$, and $[0\ 0\ 1]$ directions with an accuracy better than $\pm 0.5^\circ$. A similar accuracy of pattern placement is obtained with our lithography. Therefore, the angular alignment of each ray with the respect to the $[1\ 0\ 0]$ (or $[0\ 1\ 0]$) direction is known to an accuracy of $\pm 1^\circ$. This accurate alignment and the reasonably fine angular separation between the rays enable precise measurement of the angle-resolved electrical transport for each thin film sample.

4. Results

Representative $\rho(\phi)$ and $\rho_T(\phi)$ data are shown in Fig. 2 for an LSCO ($p = 0.04$) film at the temperature $T = 30\text{ K}$. In the upper panel, the $\rho_T(\phi)$ data (solid blue circles) oscillate around zero with a period of 180° , and can be well fitted by the expression $\rho_T(\phi) = \rho_T^0 \sin[2(\phi - \alpha)]$ (solid red line) where ρ_T^0 is the amplitude and α is the phase offset. The nematic director is not aligned with the crystal lattice ($\alpha = 60^\circ$), indicating that the observed nematicity is purely electronic, as discussed in Section 2.

Download English Version:

<https://daneshyari.com/en/article/8164052>

Download Persian Version:

<https://daneshyari.com/article/8164052>

[Daneshyari.com](https://daneshyari.com)